SEAFLOOR CHARACTERISATION USING MULTIBEAM DATA: SONAR IMAGE PROPERTIES, SEABED SURFACE PROPERTIES AND ECHO PROPERTIES

ZBIGNIEW ŁUBNIEWSKI

Gdansk University of Technology, Department of Geoinformatics
11/12, G. Narutowicza St., 80-952 Gdansk, Poland
lubniew@eti.pg.gda.pl

In the paper, the approach to seafloor characterisation is presented. The multibeam sonars, besides their well verified and widely used applications like high resolution bathymetry and underwater object detection and imaging, are also the promising tool in seafloor characterization and classification, having several advantages over conventional single beam echosounders. The proposed approach relies on the combined, concurrent use of several techniques of multibeam sonar data processing. The first one is based on constructing the grey-level sonar images of seabed using the backscattering strength calculated for the echoes received in the consecutive beams. Then, the set of parameters describing the local region of sonar image is calculated. These include both the first and the second order statistics of the grey level, and the texture analysis. The second technique utilises the 3D model of the seabed surface, which is constructed as a set of (x, y, z) points using the detected bottom range for each beam in the multibeam system seafloor imaging procedure. For the local region of seabed surface, the descriptors like rms height and autocorrelation radius are calculated. The third technique assumes the use of a set of parameters of the multibeam echo envelope, similarly as in single beam classification. The parameters include echo energy and its statistics, as well as the set of echo shape descriptors, and are calculated for each beam allowing the estimation of their dependence on seafloor incident angle. Then, for selected parameters, the characteristic features quantitatively describing their angular dependence, like slope, or range, are calculated. Finally, the features obtained by these 3 techniques have been combined together and used in seabed supervised classification procedure based on standard classifiers. The proposed method has been tested using multibeam data records acquired from several bottom types in the Gulf of Gdańsk region. The obtained results show that application of the proposed combined approach improves the classification performance in comparison with those of using only the one scheme of seafloor multibeam data processing.

INTRODUCTION

The multibeam sonars, besides their well verified and widely used applications like high resolution bathymetry and underwater object detection and imaging, are also the promising

tool in seafloor characterisation and classification, having several advantages over conventional single beam echosounders. However, the efficient and reliable methods of multibeam data processing for seabed classification have not been stated and verified yet.

The proposed approach relies on the combined use of three different techniques. The first one, introduced by the authors lately [1], is based on constructing the grey-level sonar images of seabed extracted from echoes received in the consecutive pings. Then, the set of parameters describing the local region of sonar image is calculated. The second technique utilises the 3^D model of the seabed surface, which is constructed as a set of (x, y, z) points using the detected bottom range for each beam. For the local region of the obtained seabed surface model, the descriptors like rms height and autocorrelation radius are calculated. The third technique, also introduced by the authors [2], assumes the use of a set of parameters of the multibeam echo envelope and investigating the dependence of their values on the beam incident angle.

1. MATERIALS AND METHODS

The scheme of the applied approach was shown in Fig. 1. In the first technique, i.e. Method 1 in Fig. 1, the grey-level sonar images of seabed surface are utilised, like, for instance, in [3]. Usually, such images are generated by a multibeam sonar firmware. Next, a set of parameters describing the local region of sonar image is calculated for each bottom type. This step includes calculation of the following:

1. Basic statistical parameters describing the grey level distribution, i.e. local mean, standard deviation (*STD*), skewness, and kurtosis.
2. Slope of the autocorrelation function of a grey level (in along track direction) approximated for a local region of the image (*SL_AUTC*).
3. Parameters used in the texture analysis based on the Grey-Level CO-occurrence Matrix (GLCM) of a sonar image local region: entropy (*ENTR*) and local homogeneity (*HOMOG*). The description of this technique may be found for instance in [4].

In the second technique of multibeam sonar data processing (Method 2 in Fig. 1), the 3^D model of the seabed surface is utilised. It is constructed as a set of (x, y, z) points using the detected bottom range for each beam within the multibeam system seafloor imaging procedure. Next, for the local region of the constructed seabed surface, the following descriptors are calculated: rms height (*SURF_RMS*), skewness of height (*SURF_SKEW*), kurtosis of height (*SURF_KURT*), and the slope of the seabed surface autocorrelation function (*SURF_AUTC*).

In the third technique of multibeam sonar data processing (Method 3 in Fig. 1), the set of echo signal envelopes corresponding to particular beams is obtained as a multibeam sonar output. After detection of a bottom echo in the received signal, the set of echo parameters is calculated for an appropriate part of each beam echo [2]. In the presented work, two echo parameters are used in further processing, namely:

1. The normalised moment of inertia I [5] of the echo envelope, with respect to the axis containing its gravity center.
2. Fractal dimension D of an echo envelope, interpreted as a measure of its shape composedness. It is calculated as a box dimension approximation of a Haussdorff dimension, as described in [2].

Next, for each seabed type, the dependence of I and D parameter values on the beam incident angle is estimated. The estimated angular dependences for a set of multibeam echo parameters may be found in [2].

In the context of the classification procedure construction and testing, the following quantities are calculated in the next step for each sounding (swath), based on the I and D angular dependencies:

- the approximated slope of the angular dependence of the beam echo moment of inertia $I(\varphi)$, for the angle range of [2°, 17°],
- the approximated slope of the angular dependence of the beam echo fractal dimension $D(\varphi)$, for the angle range of [4°, 19°].

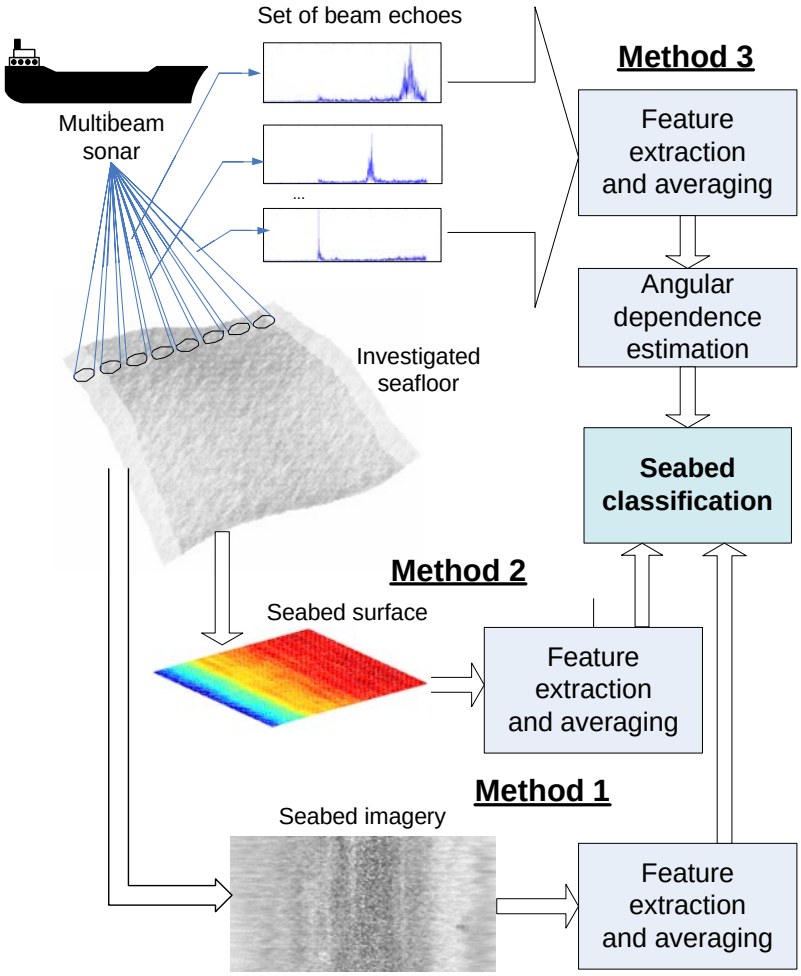

Fig. 1. The concept of three combined methods of seafloor classification using multibeam sonar

Finally, using the results obtained by both techniques described above, the 2^D plots of calculated values for selected pairs of echo or image parameters were constructed. The obtained results are presented in the next section.

The data used in the experimental verification of the proposed approach were acquired by the Kongsberg EM 3002 sonar in the Gdańsk Bay region of the Baltic Sea in September 2007. Several sites of different seabed types were investigated, but the results of the current investigation are presented and discussed for 4 selected data measure sites corresponding to 4 seabed types: mud, anthropogenic sand and mud, fine grained sand and coarse grained sand. The information about seafloor type was taken from the geological map of the Gdańsk Bay.

The sonar operating frequency was 300 kHz, the width of beams: 1.5° x 1.5°, the transmitted pulse length: 0.15 ms, the echo sampling rate: 14.3 kHz. The bottom depth was in a range between 10 m and 100 m. Approximately, 1000 swaths from each of four seafloor types were processed. For each swath, 160 beams covered the angle sector from –65° to 65°. In the first ('image') technique, the seabed sonar image part corresponding to the beam angle sector between 15° and 30° was selected for processing. In the estimation of mean, standard deviation, skewness and kurtosis of an image grey level, the size of a local image region was chosen as 11 x 11 pixels. The same local region size was used for entropy and local homogeneity calculation based on GLCM. For GLCM calculation, the image was quantised on 10 grey levels. In the estimation of the autocorrelation function slope, the used window size was 61 pixels and the maximum lag was 3 pixels. In the second technique of sonar data processing, the seabed surface part corresponding to the beam angle sector between 15° and 50° was selected for processing. In the estimation of rms height, skewness and kurtosis, the size of a local image region was chosen as 11 x 21 pixels. In the estimation of seabed surface autocorrelation function slope, the used window size was 21 pixels and the maximum lag was 3 pixels. In the third technique, i.e. echo parameter angular dependence estimation, the beam echoes corresponding to angular sector from –25° to 25° were selected for further processing and parameter calculation.

2. RESULTS

The 2^D plots of selected pairs of parameter values are presented in Fig. 2 with true seabed type of a single data point indicated by colour and shape. The 2^D plot of the (*STD*, *SL_AUTC*) pairs is presented in Fig. 2a. The plot of the (*ENTR*, *HOMOG*) pairs calculated using GLCMs technique is presented in Fig. 2b. The 2^D plot of the (*SURF_RMS, SURF_AUTC*) pairs is presented in Fig. 2c. The plot of the (*SURF_SKEW*, *SURF_KURT*) pairs is presented in Fig. 2d. The 2^D plot of the ($I(\varphi)$ slope, $D(\varphi)$ slope) pairs calculated using multibeam echoes is presented in Fig. 2e.

For comparison, the calculated values of the echo duration time *T* for normal incidence as well as of the echo energy *E* for normal incidence for the data from the same soundings, was also analysed in the similar way as other results. The results for these quantities, corresponding to those used often in the single beam seabed classification, are presented in a 2^D plot of the ($T(0°)$, $E(0°)$) pairs in Fig. 2f.

Finally, Fig. 3 presents of $I(\varphi)$ slope calculation results combined with *SL_AUTC* calculation results, e.g. one 'echo' parameter combined with one 'image' parameter. It is visible that in Fig. 2a), b), c) and e) cases, and especially in the case presented in Fig. 3, the seabed classes are separable easier than in a normal incidence parameters $T(0°)$, $E(0°)$ case – Fig 2f. It proves the advantages of the presented novel approaches.

It is visible that in the cases shown in Fig. 2a), b), c), d) and e), the distinction between some pairs of seabed types (classes) is easier, while for others it is more difficult. It may be also noticed that *ENTR* and *HOMOG* are highly, negatively correlated with each other, what is quite understandable.

It must be pointed out that while using the 'echo' ($I(\varphi)$ slope, $D(\varphi)$ slope) pair of parameters (what has already been presented partially in [2]) allows for very good separation of mud from 3 other seabed types – Fig. 2e), at the same time, using the 'image' parameter (*STD*, *SL_AUTC*) pair (Fig. 2a) makes it possible to distinct clearly between anthropogenic sand and mud and the other types, especially due to differences in local autocorrelation slope values.

Finally, using the $I(\varphi)$ slope combined with the *SL_AUTC* calculation results, i.e. one 'echo' parameter combined with one 'image' parameter, allows for very good separation of almost

all seabed classes, with the only exception of fine grained sand mixed with coarse grained sand – Fig. 6. However, these two bottom types are very similar to each other.

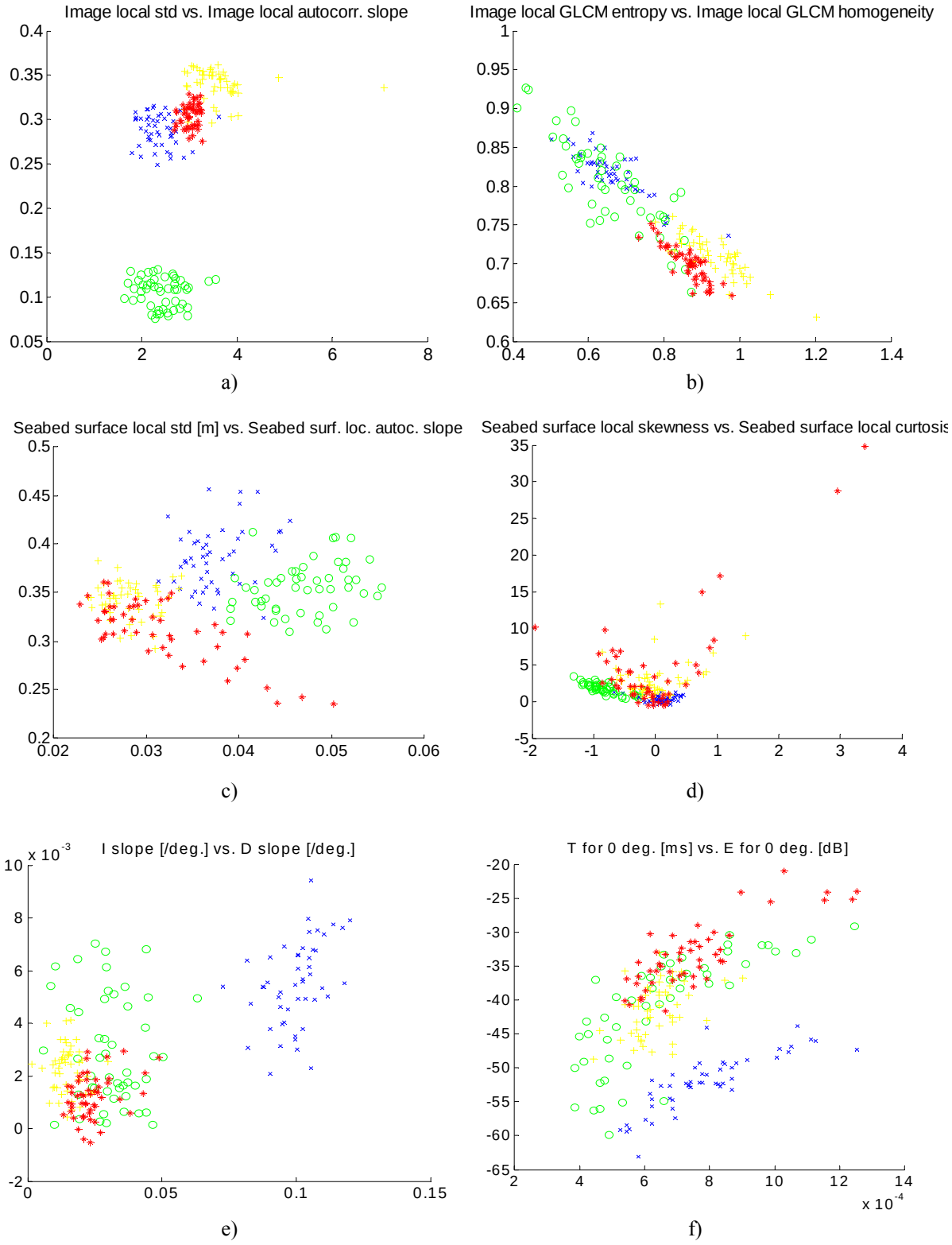

Fig. 2. 2^D plots of pairs of calculated parameter values for 4 investigated seabed types: mud x letters), anthropogenic sand and mud (circles), fine grained sand (crosses) and coarse grained sand (stars)

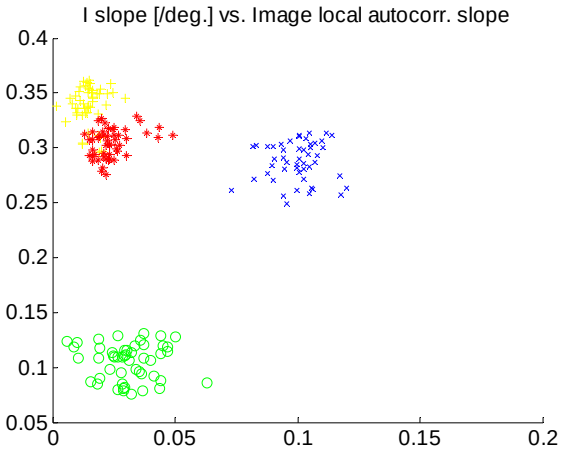

Fig. 3. 2^D plots of ($I(\varphi)$ slope, *SL_AUTC*) calculated parameter values for 4 investigated seabed types: mud (x letters), anthropogenic sand and mud (circles), fine grained sand (crosses) and coarse grained sand (stars)

The observations reported above were also confirmed by the results of testing of an automatic classifier operating on features selected from those presented in Fig. 2 and 3. The supervised classification procedure based on the training set containing the 20% of data for each seabed type was applied. The simple minimum distance classifier with Euclidean metrics was used. In the first 'echo' case (dataset 1), the ($I(\varphi)$ slope, $D(\varphi)$ slope) pairs were used as the descriptors of classified objects (e.g. bottom types), what corresponds with the plot in Fig. 2e. In the second 'surface' case (dataset 2), the (*SURF_RMS, SURF_AUTC*) pairs were used as the descriptors of bottom types, what corresponds with the plot shown in Fig. 2c. In the third 'image' case, (*STD*, *SL_AUTC*) pairs were used as the descriptors of bottom types, what corresponds with the plot shown in Fig. 2a. In the fourth case (dataset 4), the ($I(\varphi)$ slope, *SL_AUTC*) pairs were used as the descriptors of bottom types – the plot shown in Fig. 3. Finally, in the fifth case (dataset 5), the number of parameters describing the single object was extended to 3, namely, the triplet ($I(\varphi)$ slope, *STD*, *SL_AUTC*) was used.

The classification results for the dataset 1, 2, 3, 4 and 5 are presented in the form of confusion matrices in Table 1, 2, 3, 4 and 5 respectively.

Table 1. Confusion matrix for minimum distance classification of 4 seabed types using the data presented in Fig. 2e ($I(\varphi)$ slope and $D(\varphi)$ slope) as features, with 20% of data treated as the training set

Assigned class / **True class**	**Mud**	**Anthr. sand and mud**	**Fine grained sand**	**Coarse grained sand**
Mud	**100%**	0%	0%	0%
Anthr. sand and mud	1.25%	**43.75%**	7.5%	47.5%
Fine grained sand	1.25%	17.5%	**50%**	31.25%
Coarse grained sand	0%	15%	15.25%	**68.75%**
Correct classifications – total: 65.63%				

Table 2. Confusion matrix for minimum distance classification of 4 seabed types using the data presented in Fig. 2c (*SURF_RMS, SURF_AUTC*) as features, with 20% of data treated as the training set

Assigned class / **True class**	**Mud**	**Anthr. sand and mud**	**Fine grained sand**	**Coarse grained sand**
Mud	**98.75%**	1.25%	5%	6.25%
Anthr. sand and mud	0%	**70%**	13.75%	37.5%
Fine grained sand	1.25%	12.5%	**68.75%**	8.75%
Coarse grained sand	0%	16.25%	12.5%	**47.5%**
Correct classifications – total: 71.25%				

Table 3. Confusion matrix for minimum distance classification of 4 seabed types using the data presented in Fig. 2a (*STD* and *SL_AUTC*) as features, with 20% of data treatedas the training set

Assigned class / **True class**	**Mud**	**Anthr. sand and mud**	**Fine grained sand**	**Coarse grained sand**
Mud	**92.5%**	0%	0%	7.5%
Anthr. sand and mud	0%	**100%**	0%	0%
Fine grained sand	0%	0%	**86.25%**	13.75%
Coarse grained sand	5%	0%	1.25%	**93.75%**
Correct classifications – total: 93.13%				

Table 4. Confusion matrix for minimum distance classification of 4 seabed types using the data presented in Fig. 3 ($I(\varphi)$ slope and *SL_AUTC*) as features, with 20% of data treated as the training set

Assigned class / **True class**	**Mud**	**Anthr. sand and mud**	**Fine grained sand**	**Coarse grained sand**
Mud	**100%**	0%	0%	0%
Anthr. sand and mud	0%	**100%**	0%	0%
Fine grained sand	1.25%	0%	**83.75%**	15%
Coarse grained sand	0%	0%	8.75%	**91.25%**
Correct classifications – total: 93.75%				

Table 5. Confusion matrix for minimum distance classification of 4 seabed types with application of triplets of features: $I(\varphi)$ slope, *STD* and *SL_AUTC*, with 20% of data treated as the training set

Assigned class / **True class**	**Mud**	**Anthr. sand and mud**	**Fine grained sand**	**Coarse grained sand**
Mud	**100%**	0%	0%	0%
Anthr. sand and mud	0%	**100%**	0%	0%
Fine grained sand	1.25%	0%	**90%**	8.75%
Coarse grained sand	0%	0%	1.25%	**98.75%**
Correct classifications – total: 97.19%				

The obtained classification results are in line with expectations which can be made according to contents of the plots shown above. The worst classification result was in the case of the dataset 1 – 65.63% total correct classifications. It is connected with quite strong overlapping of ($I(\varphi)$ slope, $D(\varphi)$ slope) values distributions for 3 of 4 seabed types – Fig. 2e. For the dataset 2 case – (*SURF_RMS, SURF_AUTC*) pair, the results are slightly better – 71.25% total correct classifications. In this case, one may predict that the use of more advanced classification algorithm could improve the classification results. For the dataset 3 case, i.e. with the use of (*STD* and *SL_AUTC*) parameters describing the local properties of a sonar image grey level, the classification results are significantly better – 93.13% correct classifications. The further improvement of the classification performance is visible with respect to the results obtained for the dataset 4, where the combination of one 'echo' and one 'image' parameter is used. Although the total percentage of the correct classifications: 93.75% is not significantly higher than in the previous case, it should be noticed that two bottom types – mud and anthropogenic sand and mud, are classified with 100% correctness even with such a primitive type of a classifier used. This is due to very good separation of those 2 seabed classes. Finally, the best classification result was obtained in the dataset 5 case: 97.19% total correct classifications. In this case, the classification was performed in the 3-dimensional parameter space, containing one 'echo' and two 'image' parameters.

3. CONCLUSIONS

The approach to multibeam seafloor characterisation, which relies on the combined, concurrent use of three different techniques of multibeam sonar data processing, was presented. It has been primarily justified that all techniques are useful in seafloor characterisation. What is more, the obtained results show that the combination of two techniques – signal processing, and image processing, improves the seabed classification performance. However, it should be pointed out that in this investigation, the processed experimental datasets were not too large, and the information about seafloor type was obtained using the geological map of the region, which is characterised by a poor spatial resolution. To obtain more accurate results, the verification of the proposed approaches with use of larger amount of experimental data, as well as with application of a more reliable ground truthing, is needed.

REFERENCES

[1] Łubniewski Z., Stepnowski A., Chybicki A., Seafloor characterisation combined approach using multibeam sonar echo signal processing and image analysis, Proceedings of the 10th European Conference on Underwater Acoustics, Istanbul 2010, pp. 131–137.

[2] Łubniewski Z., Chybicki A., Using angular dependence of multibeam echo features in seabed classification, Proceedings of the 9th European Conference on Underwater Acoustics, Paris 2008, pp. 717–722.

[3] Preston J. M., Christney A. C., Beran L. S., Collins W. T., Statistical seabed segmentation – from images and echoes to objective clustering, Proceedings of the 7th European Conference on Underwater Acoustics, Delft 2004, pp. 813–818.

[4] Łubniewski Z., Bruniecki K., Seafloor characterisation and imaging using multibeam sonar data, 31th International Symposium on Acoustical Imaging, Warsaw 2010.

[5] Tęgowski J., Łubniewski Z., Application of some echo parameters to the seabed classification – methodological analysis, Hydroacoustics, 4, (2001), 237–240.